Journal of Molecular Structure 1180 (2019) 665–675

Contents lists available at ScienceDirect

Journal of Molecular Structure

journal homepage: http://www.elsevier.com/locate/molstruc

Structural and vibrational properties of pentabromophenol and pentafluorophenol: A spectroscopic investigation using density functional theory

P. Venkata Ramana Rao [a], K. Srishailam [a], L. Ravindranath [b], B. Venkatram Reddy [c, *], G. Ramana Rao [c]

[a] Department of Physics, S R Engineering College (Autonomous), Warangal 506371, Telangana, India
[b] Department of Physics, New Science Degree and P.G. College, Warangal 506001, Telangana, India
[c] Department of Physics, Kakatiya University, Warangal 506009, Telangana, India

ARTICLE INFO

Article history:
Received 3 October 2018
Received in revised form
5 December 2018
Accepted 10 December 2018
Available online 14 December 2018

Keywords:
Pentabromophenol
Pentafluorophenol
Vibrational spectra
Inter-molecular hydrogen bond
DFT

ABSTRACT

Fourier Transform Raman and Fourier Transform infrared spectra were measured in the spectral range 3500-100 cm^{-1} and 4000-400 cm^{-1}, respectively, for Pentabromophenol (PBP) and Pentafluorophenol (PFP). Torsional potentials, optimized structure parameters, harmonic vibrational frequencies, general valance force field, potential energy distribution (PED), along with infrared and Raman intensities were evaluated, for PBP and PFP. DFT was used in conjunction with B3LYP functional with 6–311++G (d,p) basis set, for the computations. Scaling process was employed to get a better fit between the measured and computed frequencies. The rms error between them was 9.7 and 7.0 cm^{-1}, for PBP and PFP, respectively. Unambiguous vibrational assignments were arrived at by using PED and eigenvectors. In order to substantiate the existence of inter-molecular hydrogen bond in these molecules geometry optimization was made for dimers of PBP and PFP, at the same level of theory as used for the monomers.

1. Introduction

Pentabromophenol (PBP) is finding increasing applications in the fields of agriculture and pharmaceuticals, along with pentachlorophenol [1,2]. However, investigations on PBP, both experimental and theoretical, have been very limited. It was one of the nineteen bromophenols investigated theoretically for understanding molecular structure and property relationships [3]. A tentative account of all vibrational frequencies of PBP was given by Faniran for the first time [4]. He reported the vibrational fundamentals of Pentafluorophenol (PFP) also [5]. The structure of PBP, as determined from X-ray methods, is also available [6]. But no theoretical work on PBP and PFP is available from literature to the best of our knowledge. Hence, as a continuation of our recent work on Pentachlorophenol and Pentachlorothiophenol [7], we undertook this work with the following aims.

To record FT-IR, and FT-Raman, spectra of PBP and PFP, and
To perform DFT calculations on the molecules so as to,

(i) identify the most stable rotational conformer by obtaining torsional potentials for various angles of rotation around the C–O bond,
(ii) optimize equilibrium geometry for the stable rotational isomer and its dimer, and
(iii) compute harmonic vibrational frequencies and their IR and Raman intensities.

2. Measurement of spectra

Pure sample of solid PBP was purchased from Tokyo Kasei Kogyo Co. Ltd, Japan, and that of PFP was obtained from Aldrich Chemical Company (USA). They were used, as such, for spectral measurements.

Fourier Transform IR (FT-IR) spectrum of PBP and PFP was recorded, in the spectral range 4000-400 cm^{-1}, using Nicolet-740 single beam spectrometer equipped with liquid nitrogen-cooled Deuterated Triglycine Sulphate (DTGS) detector, by diluting the sample in KBr pellet. As PFP was a liquid at room temperature, its spectrum was measured by squeezing in a thin film of unknown

* Corresponding author.
E-mail address: bvreddy67@yahoo.com (B.V. Reddy).

https://doi.org/10.1016/j.molstruc.2018.12.036
0022-2860/

thickness between two plates of KBr. The spectra were a result of co-addition of 32 scans.

Fourier Transform Raman (FT-Raman) spectra of the same samples were measured with RFS 100 FT-Raman spectrometer, equipped with Ge diode detection system in the 3500-100 cm^{-1} Stokes region. Nd-YAG laser operating at 200mw power provided the exciting radiation at 1064 nm. The spectra were a result of co-addition of 256 scans.

3. Computational details

All computations were accomplished by means of the Gaussian 09/DFT PROGRAM package [8]. Beck's three parameter hybrid exchange functional B3 [9] along with Lee-Yang-Parr (LYP) correlation functional [10], employing the valence triple basis set i.e. 6-311++G (d, p) was used. The reasons for using the above combination of functionals and basis set were the following. It was shown by Rauhunt and Pulay [11] that B3LYP functional gave frequencies that are in better agreement with experimental results than the Hartree-Fock results. We found that the combination of B3LYP functional and 6-311++G (d,p) basis set yielded very good results not only for closely related systems namely Pentachlorophenol and Pentachlorothiophenol [7] but also for a relatively complex systems of bipyridines [12]. Further, Karabacak et al. [13] successfully employed this combination of functional and basis set for computing structural and vibrational parameters of 5-fluoro- and 5-chloro-salicylic acid.

C—O is the only bond around which rotation is permitted in PBP or PFP. Hence to find rotational conformer of lowest energy, torsional potential energy was computed as a function of angle of rotation around the C—O bond in steps of 10° between 0° and 360°. This yielded two −fold potential barrier with minimum energy at 0° for both PBP and PFP. The lowest energy conformer was subjected to rigorous preliminary geometry optimization with simultaneous relaxation of all structural parameters. Following standard procedure, the initial geometrical parameters required for the optimization were taken from X-ray studies for PBP [6], whereas they were transferred from closely related systems namely Pentafluoroaniline [14] and hydrogen bonded complex between PFP and tryphenylphosphine oxide [15] for PFP (for details see Table 1), as the same are not available for PFP. This process led to planar structure, which almost remained unchanged in the final optimization, yielding planar structure of C_s symmetry.

C_S planar structure was used as equilibrium reference geometry. Vibrational Cartesian force constants, harmonic vibrational wavenumbers, and the dipole moment along with its derivatives, were computed first for PBP and PFP. In all further calculations, the reference geometry and corresponding force constants were taken as initial data. The force constants were transformed using MOLVIB 7.0 program [16,17] into a non-redundant set of 33 natural internal coordinates (i.e. local symmetry coordinates) consisting of thirteen bond stretchings (6 CC, 5 CBr or CF, 1 CO, and 1OH), ten ring in-plane bendings (5 CBr or CF, 1CO, 1OH and 3 ∠CCC), four torsions (1 OH, or 3 ∠CCCC) and six out-of -plane waggings (5 CBr or CF and 1 CO) obtained from 46 redundant internal coordinates (i.e. primitive internal coordinates) made up of thirteen bonds (6 CC, 5CBr or CF, 1 CO and 1 OH), nineteen angles (10 ∠CCBr or CCF, 2 ∠CCO, 6 ∠CCC, 1 ∠COH), eight torsions (2 OH, 6 ∠CCCC) and six waggings (5 CBr or CF and 1 CO), according to the recommendations of Fogarasi et al. [18]. In order to ensure a better fit of observed and calculated frequencies, the force constants were scaled using empirical scaling factors employing multiple scaling method of Fogarasi and Pulay [19] and Arenas et al. [20] with least-square refinement of the scale factors, wherein the calculated normal frequencies of PBP or PFP were fitted to their experimentally ascribed vibrational fundamentals. In order to characterize the normal modes we computed potential energy distribution (PED), and relative IR absorption intensities [21], relative Raman scattering intensities [22,23], in addition to obtaining fundamental frequencies and corresponding eigenvectors. To understand the nature of intermolecular hydrogen bond in PBP and PFP, their dimers were subjected to geometry optimization, at the same level of theory as the corresponding monomer. IR and Raman spectra were simulated for PBP and PFP using a pure Lorentzian band shape with full width at half maximum (FWHM) of 10 cm^{-1}, in order to compare them with corresponding experimental spectra recorded by us.

4. Results and discussion

4.1. Barrier to internal rotation

The two-fold potential barriers obtained for PBP and PFP, as explained in section 3, are shown graphically in Fig. 1. This figure represents the plot of relative energy vs angle of rotation, where relative energy stands for energy of each rotamer with respect to the rotamer of lowest energy. From this figure it can be seen that there are two barriers to internal rotation for PBP and PFP, each, one situated between 0° and 180° and the other between 180° and 360°, in one complete rotation around the C—O bond in these molecules. The height of the barrier hindering internal rotation, around C—O bond in PBP and PFP is obtained as the difference between the energies of the point of lowest energy and the point of highest energy known as transition state [24], in Fig. 1. They occur at rotational angle of 0° and 90°, respectively, in both PBP and PFP. The respective energy differences are 0.007126 Hartree (18.70 kJ mol^{-1} or 4.47 kcal mol^{-1}) and 0.004775 Hartree (12.54 kJ mol^{-1} or 3.00 kcal mol^{-1}) for PBP and PFP. This is the same as 1563 and 1049 cm^{-1} for PBP and PFP, respectively. The value calculated for PBP compares very well with its counterpart reported by Faniran [4] at 1447 ± 6 cm^{-1}, but the deviation is much higher for PFP as the barrier value reported by Faniran [5] is 1273 cm^{-1}. It is important to note here that the experimental barrier heights depend on structure parameters and corresponding torsional frequency [4], whereas the main source of error in the B3LYP method comes from a systematic underestimation of the classical barrier height [25]. As in phenol [26] the barrier arises due to conjugation between π−electrons of the benzene nucleus and lone pair on oxygen atom in PBP and PFP, imparting partial double bond character to the C—O bond.

4.2. Molecular geometry of the most stable conformer

Optimized geometry generated by solving self-consistent field equations iteratively, for PBP and PFP, is shown in Fig. 2. Corresponding geometry for the dimers appear in Fig. 3. The same figures contain numbering of atoms also. Values of optimized structure parameters comprising of bond lengths, bond angles and dihedral angles of PBP and PFP are presented in Table 1, along with their corresponding experimental values [6,25,26], for both monomers and dimers. Experimental values in the case of PFP are taken from the corresponding values of Pentafluoroaniline [14] and hydrogen bonded complex between PFP and triphenylphospine oxide [15], as the same are not available for PFP.

4.2.1. Monomer and intra-molecular hydrogen bonding

As explained in section 3, planar configuration of C_S symmetry is preferred by both PBP and PFP. This is a result of conjugation between π -electrons of the benzene ring and two lone pairs in the oxygen atom of hydroxyl moiety. From Table 1, it can be seen that

Table 1
Experimental and DFT/B3LYP/6-311++G (d,p) optimized geometric parameters of pentabromophenol (PBP), pentaflurophenol (PFP) and their dimers.

Geometric parameter	PBP			PFP		
	Calculated value		Experimental[a]	Calculated value		Experimental[b]
	Monomer	Dimer		Monomer	Dimer	
Bond lengths (in Å)						
C1–C2	1.402	1.401	1.395	1.395	1.392	1.390
C2–C3	1.398	1.398	1.387	1.389	1.389	1.379
C3–C4	1.406	1.407	1.391	1.391	1.391	1.381
C4–C5	1.403	1.403	1.390	1.389	1.390	1.384
C5–C6	1.397	1.398	1.393	1.387	1.387	1.377
C6–C1	1.401	1.400	1.389	1.393	1.391	1.397
C1–O7	1.345	1.350	1.360	1.352	1.362	1.348[c]
C2–Br9	1.899	1.898	1.884	*	*	*
C3–Br10	1.900	1.904	1.888	*	*	*
C4–Br11	1.903	1.899	1.886	*	*	*
C5–Br12	1.900	1.900	1.882	*	*	*
C6–Br13	1.913	1.912	1.886	*	*	*
C2–F9	*	*	*	1.336	1.337	1.342
C3–F10	*	*	*	1.334	1.333	1.341
C4–F11	*	*	*	1.336	1.334	1.339
C5–F12	*	*	*	1.335	1.333	1.338
C6–F13	*	*	*	1.350	1.348	1.341
O7–H8	0.969	0.970	0.840	0.965	0.966	0.860[c]
Bond angle (in °)						
C1–C2–C3	120.36	120.31	120.3	120.79	120.63	122.2
C2–C3–C4	120.31	120.32	120.4	120.43	120.25	120.3
C3–C4–C5	119.56	119.49	119.7	119.53	119.70	118.9
C4–C5–C6	119.59	119.63	119.8	119.44	119.41	120.2
C5–C6–C1	121.24	121.13	120.7	121.99	121.63	122.1
C6–C1–C2	118.92	119.08	119.1	117.79	118.34	116.3
C1–C2–Br9	116.97	117.28	117.6	*	*	*
C3–C2–Br9	122.67	122.38	122.9	*	*	*
C2–C3–Br10	119.37	119.47	119.3	*	*	*
C4–C3–Br10	120.32	120.18	120.3	*	*	*
C3–C4–Br11	120.37	120.54	120.0	*	*	*
C5–C4–Br11	120.06	119.96	120.4	*	*	*
C4–C5–Br12	120.92	120.97	120.7	*	*	*
C6–C5–Br12	119.43	119.40	119.5	*	*	*
C5–C6–Br13	122.32	122.41	121.9	*	*	*
C1–C6–Br13	116.43	116.45	117.4	*	*	*
C1–C2–F9	*	*	*	119.71	119.53	118.4
C3–C2–F9	*	*	*	119.49	119.82	119.4
C2–C3–F10	*	*	*	119.83	119.89	119.9
C4–C3–F10	*	*	*	119.73	119.84	119.8
C3–C4–F11	*	*	*	120.24	120.15	120.3
C5–C4–F11	*	*	*	120.21	120.14	120.8
C4–C5–F12	*	*	*	120.27	120.32	120.1
C6–C5–F12	*	*	*	120.27	120.26	119.7
C5–C6–F13	*	*	*	120.19	120.44	119.4
C1–C6–F13	*	*	*	117.81	117.91	118.47
C6–C1–O7	122.83	120.27	122.9	122.78	122.22	123.6[c]
C2–C1–O7	118.24	118.65	117.9	119.41	119.42	118.9[c]
C1–O7–H8	109.26	108.99	109.5	109.55	109.75	112.0[c]
Dihedral angle (in °)						
C1–C2–C3–C4	0.00	2.26	0.40	0.00	0.29	–
C2–C3–C4–C5	0.00	1.87	0.00	0.00	0.14	–
C3–C4–C5–C6	0.00	0.58	−0.20	0.00	0.030	–
C4–C5–C6–C1	0.00	0.32	0.00	0.00	0.060	–
C5–C6–C1–C2	0.00	0.048	0.40	0.00	0.090	–
O7–C1–C2–Br9	0.00	0.48	0.70	*	*	*
C1–C2–C3–Br10	180.00	179.73	178.50	*	*	*
C2–C3–C4–Br11	−180.00	177.47	−179.90	*	*	*
C3–C4–C5–Br12	180.00	−179.67	179.90	*	*	*
C4–C5–C6–Br13	180.00	179.37	179.60	*	*	*
C5–C6–C1–O7	180.00	179.89	179.40	180.00	179.80	–
C6–C1–O7–H8	0.00	2.71	–	0.00	2.95	–
C2–C1–O7–H8	−180.00	−177.45	–	180.00	177.20	–
O7–C1–C2–C3	−180.00	−178.81	−179.70	*	*	*
C6–C1–C2–C3	0.00	1.34	0.60	*	*	*
Br9–C2–C3–C4	−180.00	−179.49	−180.00	*	*	*
Br9–C2–C3–Br10	0.00	1.49	1.10	*	*	*
Br10–C3–C4–C5	180.00	179.86	178.90	*	*	*
Br10–C3–C4–Br11	0.00	0.52	1.10	*	*	*
Br11–C4–C5–C6	−180.00	−178.76	−179.70	*	*	*

(*continued on next page*)

Table 1 (*continued*)

Geometric parameter	PBP			PFP		
	Calculated value		Experimental[a]	Calculated value		Experimental[b]
	Monomer	Dimer		Monomer	Dimer	
Br11–C4–C5–Br12	0.00	0.98	0.10	*	*	*
Br12–C5–C6–C1	180.00	179.43	179.70	*	*	*
Br12–C5–C6–Br13	0.00	0.88	0.70	*	*	*
O7–C1–C6–Br13	0.00	0.40	0.20	*	*	*
C2–C1–C6–Br13	180.00	179.76	179.20	*	*	*
O7–C1–C2–F9	*	*	*	0.00	0.26	–
C1–C2–C3–F10	*	*	*	180.0	179.90	–
C2–C3–C4–F11	*	*	*	180.0	179.80	–
C3–C4–C5–F12	*	*	*	180.0	180.00	–
C4–C5–C6–F13	*	*	*	180.0	179.90	–
Inter-molecular H-bond lengths and angles of dimer						
(i) PBP						
O7–H8 … O20		2.26	2.19			
O7 … O20		2.96	2.84			
O7–H8		0.97	0.84			
O7–H8 … Br26		3.38	–			
O7–H8 … O20		127.78	134.00			
O7–H8 … Br26		127.95	–			
(ii) PFP						
O7–H8 … O20		1.95	–			
O7 … O20 2.88						
O7–H8		0.97	–			
O7–H8 … F26		2.91	–			
O7–H8 … O20		160.31	–			
O7–H8 … F26		128.04	–			

*: Not relevant
-: Not available.
[a] From reference 6.
[b] From reference 14, c: From reference 15.

the computed structure parameters of PBP and PFP agree fairly well with their corresponding results of X-ray investigations [6,25,26]. For example, according to computations for PBP, the average value of C–C bond length is 1.401 Å; the average value of C–Br bond distance is 1.903 Å; and O–H bond distance is 0.969 Å. They agree extremely well with their corresponding experimental values 1.391 Å; 1.885 Å; and 0.840 Å. Noticeable deviations in the case of O–H bond distance is attributable to the inherent inability of X-ray methods to locate the position of hydrogen atom in structure determination.

Three bond angles around C1 carbon atom are expected to be affected by the presence of oxygen atom in PBP. These are ∠C6C1C2, ∠C6C1O7, and ∠C2C1O7 having computed values 118.92°, 122.83°, and 118.24°, respectively. They agree extremely well with the corresponding X-ray diffraction results of PBP [6] at 120.7°, 122.9°, and 117.9°. Similar conclusions can we drawn in respect of PFP by referring to the results in Table 1.

The distance between the lone hydrogen atom and its nearest bromine atom (Br9) in PBP is 2.393 Å, whereas the corresponding quantity in PFP is 2.278 Å (see Fig. 2), as per our calculations. From this it can be inferred that there is a weak intra-molecular hydrogen bond in these molecules.

4.2.2. Dimer and inter-molecular hydrogen bonding

It is to be stated here that dimer of PBP or PFP was treated as a supra molecule consisting of two stable monomers in their lowest energy conformation with experimental values for inter-molecular hydrogen bond. The resulting configuration was subjected to rigorous geometry optimization with simultaneous relaxation of all structural parameters as in the case of monomer. This process led to structure of C_1 symmetry for both PBP and PFP dimers. Consequently the two monomer units of the dimer do not share the same molecular plane. As the monomer and dimer are treated at the same level of theory, comparative results are expected to be reliable. Optimized geometry obtained in this way for dimers of PBP and PFP, is shown in Fig. 3. This figure contains numbering of atoms also. The optimized structure parameters of dimers of PBP and PFP are collected in Table 1, along with their corresponding monomers.

The minimum energy of PBP dimer is −26350.4798 Hartree (-69183.1900×10^3 kJ mol^{-1} or -16535.1793×10^3 kcal mol^{-1}), whereas the corresponding value for PFP dimer is −1607.7210 Hartree (-4221.0718×10^3 kJ mol^{-1} or -1008.8604×10^3 kcalmol^{-1}). For formation of dimer these energies should be less than twice the minimum energy of corresponding monomers. We find that the difference between the energy of PBP dimer and twice the energy of its monomer is −0.003586 Hartree (−9.415 kJ mol^{-1} or -2.250 kcal mol^{-1}). The corresponding quantity for PFP dimer is −0.007210 Hartree (−18.93 kJ mol^{-1} or -4.52 kcal mol^{-1}). Hence formation of dimer is favored in both PBP and PFP. It is to be stated here that basis set superposition error [27,28], which can be estimated and corrected for, by the method of counterpoise correction [29,30] is not attempted, as this effect is usually minor with large basis set used in our calculations [31].

In dimers of PBP and PFP structural configuration around atoms involved in inter-molecular hydrogen bond is of special interest (see Fig. 3). The relevant bond distances and bond angles are available in Table 1. In the case of PBP dimer hydrogen atom H8 of hydroxyl moiety of one monomer is involved in hydrogen bonding with Oxygen atom O20 (see Fig. 3) of the other monomer in the dimer. Calculated value of H8 … ••O20 hydrogen bond length is 2.260 Å. Corresponding experimental value for H8 …. O20 is 2.190 Å [6]. This agrees well with its calculated counterpart. In the case of PFP calculated H8…O20 distance is 1.949 Å. Steiner, in his marvelous review article [32], suggested a highly approximate

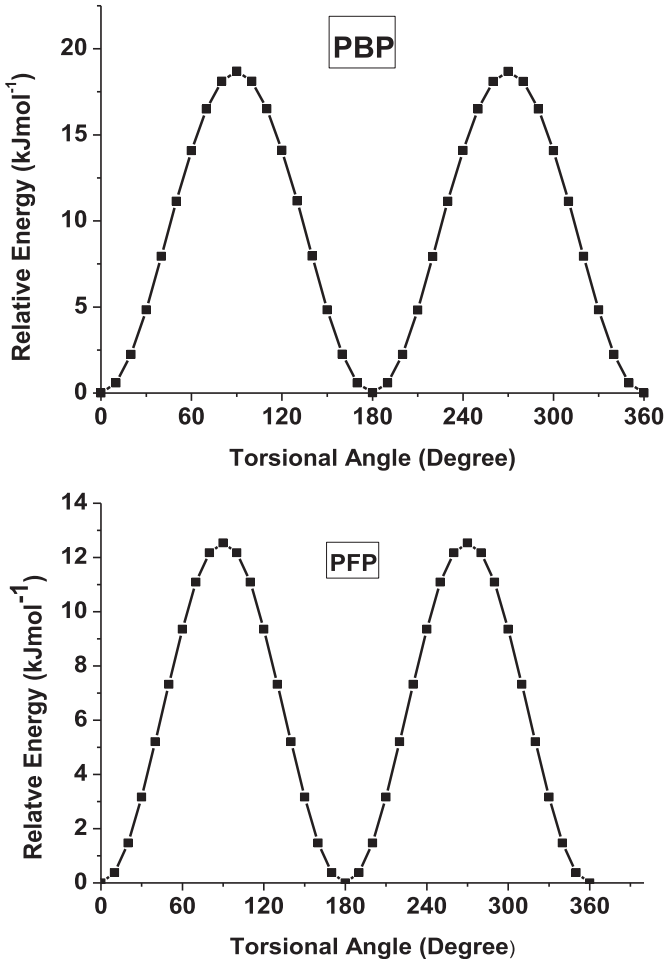

Fig. 1. Relative torsional potential energy as a function of rotational angle of PBP and PFP computed at the DFT/B3LYP level using 6-311++G (d,p) basis set.

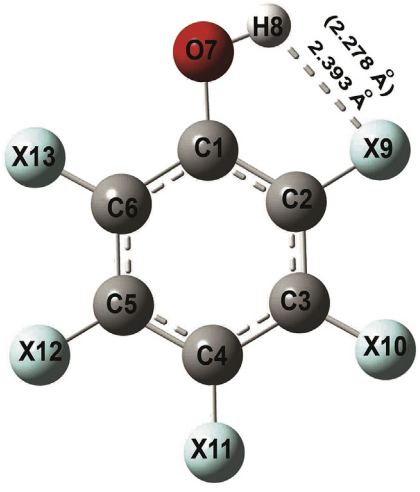

Fig. 2. Optimized molecular structure of PBP and PFP monomers showing intramolecular hydrogen bond with numbering of atoms ($E_{PBP} = -34591.5903 \times 10^3$ kJ mol^{-1} and $E_{PFP} = -2110.5265 \times 10^3$ kJ mol^{-1}) (For PBP: X = Br; For PFP: X = F. Value in braces is for PFP).

range 2.4–2.8 Å for weak hydrogen bond distances. Hence the hydrogen bond in PBP and PFP dimer is considered as strong. The distance between H8 …. Br26 of PBP is calculated to be 3.377 Å and that between H8 …. F26 distance as 2.911 Å. These are due to Vander Waals interactions arising from electrostatic forces, as both are >2.8 Å. According to Steiner [32] hydrogen bonds, in general, comprise of various kinds of interactions, but in the medium and long-distance region the electrostatic component is the dominant one. Hence it is not easy to establish where a hydrogen bond ends and a Vander Waals interaction begins as noted by Steiner and Desiraju [33,34]. However a better assessment of H-bonds interactions can be made by using Bader's theory of 'Atoms in Molecules' implemented in AIM2000 software updated by Biegler-kö nig and Schö nbohm [35] in 2002.

4.3. Scaled force constants

We have defined 33 natural internal coordinates for each of the molecules PBP and PFP. As the force constant matrix is symmetric, the number of general valence force constants is given by n (n+1)/2, where n is the number of natural internal coordinates or basis coordinates. Hence the total number of force constants for PBP or PFP is 33 × 34/2 = 561. We know that there are 23 in-plane coordinates of a'-species and 10 out-of-plane coordinates of a″-speceies, in each of the molecules under consideration. The interaction between coordinates of a′- and a″-species is symmetry-forbidden. Hence there should be 23 × 10 = 230 force constants having zero value for PBP and PFP, each, due to symmetry reasons. Hence, the expected number of non-zero force constants is 561-230 = 331. Out of these 23 × 24/2 = 276 constants belong to in-plane force constants of a′-species and 10 × 11/2 = 55 constants belong to out-of-plane force constants of a″-speceies. In fact DFT calculations generated a force field, which perfectly conforms to the foregone conclusions (i.e., 276 in-plane force constants, 55 out-of-plane force constants and 230 symmetry-forbidden force constants). Within a given species, a very small number of interaction constants have significant values; some have relatively small values; yet some others have negligibly small and zero values. To demonstrate this statement, let us consider the stretch-stretch interaction constants between C1–C2 bond of the aromatic nucleus and other stretching coordinates of PBP (see Fig. 2). Neighboring stretching coordinates to C1–C2 bond are, two ortho carbon-carbon bonds (C2–C3 and C1–C6), C–O bond, and C2–Br9 bond. The interaction constants associated with these bonds involving C1–C2 bond, as per DFT calculations are 0.723, 0.798, 0.652 and 0.423 mdyneÅ^{-1}, respectively, which are significant due to geometric proximity. The exception to proximity rule are two C–C, C–C meta- and one C–C, C–C para-interaction constants, whose values are −0.518 (C3–C4), −0.502 (C5–C6), and 0.074 mdyneÅ^{-1}, which are significant. It is note-worthy that such exception is also found for meta- and para-interaction constants (i.e, C–C, C–C) of the aromatic nucleus in the case of substituted benzenes [e.g Refs. [36–38]] obtained by solving inverse vibrational problem using Wilson's GF matrix method [39]. The O–H stretch interaction constant with C3–Br10 stretch deserves special mention, because its value is zero. This can be attributed to the geometric separation between the corresponding coordinates.

4.4. Vibrational assignments

The geometry optimization in section 3 (computational considerations) led to C_S symmetry for both PBP and PFP. PBP or PFP consists of 13 atoms. Hence it has 33 vibrational fundamentals. In C_S symmetry they are distributed as 23 in-plane vibrations of a′-species and 10 out of plane vibrations of a″-species, according to the formulae 2N-3 and N-3, respectively, where N is the number of atoms in the molecule. All the vibrations of C_S symmetry are active in both infrared absorption and Raman scattering.

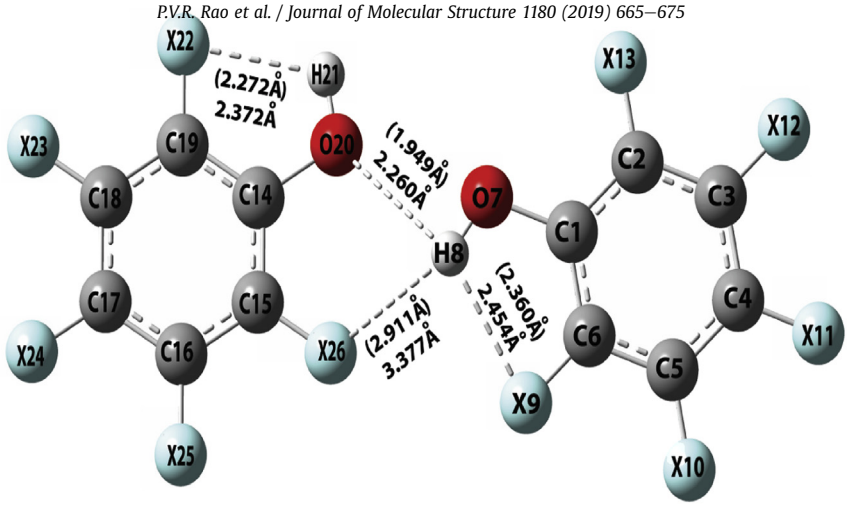

Fig. 3. Optimized molecular structure of PBP and PFP dimers showing inter-molecular and intra-molecular hydrogen bonds with numbering of atoms ($E_{PBP} = -69183.1900 \times 10^3$ kJ mol^{-1} and $E_{PFP} = -4221.0718 \times 10^3$ kJ mol^{-1}) (For PBP dimer: X = Br; For PFP dimer: X = F. Value in braces is for PFP).

Table 2
Observed frequencies, DFT/B3LYP/6-311++G (d,p) computed frequencies along with intensities and vibrational assignment of PBP.

Mode[a]	Obs. freq.(cm^{-1})		Cal. freq. (cm^{-1})		Intensity[b]		Vibrational Assignment[c]
	IR	Raman	Unscaled	Scaled	IR (I_i)	Raman (A_i)	
(i) Vibrations of Phenol ring							
(a) In-plane vibrations(a′-species)							
ν(C–C) 8a	1533 ms	–	1558	1530	2.81	42.63	68 (8a)+8 (6b)+8 [β(OH)]+6 (15)+6 (18b)
ν(C–C) 8b	1514 vs	1524 (17)	1546	1518	17.65	82.51	72 (8b)+9 (6b)+7 (18b)
ν(C–C) 14	1278 vs	–	1292	1280	31.16	10.69	73 (14)+18 [β(OH)]
ν(C–C) 19a	1349 vs	–	1366	1348	100	6.32	53 (19a)+14 (18a)+11 (13)+10 [β(OH)]+7 (7a)
ν(C–C) 19b	1388 s	1392 (5)	1407	1377	41.85	12.91	55 (19b)+16 (13)+14 (18a)+7 [β(OH)]+5 (7b)
ν(C–Br) 2	–	237 (79)	233	235	0.01	15.16	72 (2)+16 (1)+12 (6a)
ν(C–Br) 7a	–	–	383	376	0.04	10.98	42 (7a)+30 (12)+15 (18a)+9 (1)
ν(C–Br) 7b	776 ms	–	800	783	0.09	0.03	56 (7b)+39 (6a)
ν(C–Br) 20a	682 s	–	680	670	19.64	5.18	55 (20a)+25 (6a)+10 (18a)
ν(C–Br) 20b	557 s	–	549	565	9.77	0.14	51 (20b)+48 (3)
β(CBr) 3	631 ms	633 (2)	630	632	11.14	0.26	51 (3)+35 (15)+10 (2)
β(CBr) 9a	–	140 (61)	137	138	0.04	2.06	93 (9a)
β(CBr) 9b	–	140 (61)	140	141	0.08	0.74	86 (9b)+6 (14)
β(CBr) 18a	–	152 sh (20)	144	144	0.07	0.30	84 (18a)+7 (14)
β(CBr) 18b	–	152 sh (20)	152	152	0.00	0.33	97 (18b)
ν(C–C) 1	1223 ms	1228 (6)	1233	1219	18.62	39.39	63 (1)+15 (2)+10 (3)+7 (18a)
β(CCC) 6a	–	210 sh (21)	206	199	0.03	5.13	49 (2)+40 (6a)+7 (1))
β(CCC) 6b	–	222 vs	218	215	0.02	8.47	55 (6b)+38 (7b)
β(CCC) 12	1000[d] w	–	1077	1035	0.53	6.71	35 (12)+28 (20a)+18 (1)+17 (13)
ν(C–O) 13	925 s	937 (5)	932	894	10.49	9.69	42 (6b)+38 (20a)+13 (13)+5 (1)
β(CO) 15	–	320 (9)	319	319	0.28	0.51	48 (3)+37 (15)+7 (7a)+6 (14)
(b) Out-of plane vibrations (a''-species)							
τ(CCCC) 4	698 ms	–	639	697	0.75	1.20	50 (5)+32 (4)+18 (10b)
τ(CCCC)16a	600 ms	–	581	599	0.00	1.04	52 (17a)+48 (16a)
τ(CCCC)16b	557 s	–	540	559	0.27	0.17	61 (17b)+38 (16b)
π(CBr) 11	–	152 sh (20)	159	165	0.00	0.09	78 (11)+19 (4)
π(CBr) 17a	–	–	38	38	0.00	0.00	85 (16a)+6 (17a)
π(CBr) 17b	–	–	42	42	0.00	0.04	83 (16b)+15 (17b)
π(CBr)10a	–	320 (9)	305	317	0.42	0.04	97 (10a)
π(CBr) 10b	–	347 (5)	330	342	0.60	0.07	74 (10b)+19 (4)+6 (5)
π(CO)5	-	88[d] w	84	84	0.00	0.29	73 (4)+19 (17a)+6 (5)
(ii) Vibrations of OH moiety							
(a) In-plane vibrations (a′-species)							
ν(OH)	3530[d] vw	–	3706	3530	58.08	100	100 [ν(OH)]
β(OH)	1192 vs	1195 (4)	1207	1193	58.52	17.72	61 (14)+21 [β(OH)]+6 (20b)+6 (13)
(b) Out-of plane vibrations (a''-species)							
τ(OH)	–	401 (21)	445	402	34.55	2.30	91 [τ(OH)]

-: Not observed.
vs: very strong; s: strong; ms: medium strong; w: weak; vw: very weak; sh: shoulder.
[a] Mode in Wilson's notation [40]. ν, stretching; β, in-plane bending; π, out-of-plane bending; τ, torsion.
[b] Relative infrared and Raman intensities are normalized to 100.
[c] Number before the parenthesis is % PED and number in the parenthesis is vibrational mode. PED less than 5% is not shown.
[d] From reference 4.

Table 3
Observed frequencies, DFT/B3LYP/6-311++G (d,p) computed frequencies along with intensities and vibrational assignment of PFP.

Mode[a]	Obs. freq.(cm^{-1})		Cal. freq. (cm^{-1})		Intensity[b]		Vibrational Assignment[c]
	IR	Raman	Unscaled	Scaled	IR (I_i)	Raman (A_i)	
(i) Vibrations of Phenol ring							
(a) In-plane vibrations(a′-species)							
ν(C–C) 8a	–	1662 (17)	1680	1653	5.09	20.71	65 (8a)+12 (6b)+9 (18b)+9 (13)
ν(C–C) 8b	1619 s	1622 (2)	1669	1636	0.61	9.10	65 (8b)+11 (6a)+9 (20a)+6 (3)+ 6 [β(OH)]
ν(C–C) 14	1356 vs	1364 (2)	1349	1356	33.71	3.56	45 [β(OH)]+41 (14)+7 (2)
ν(C–C) 19a	1523 vs	1514 (5)	1531	1516	100	0.10	47 (19a)+29 (20b)+9 (18b)+6 (13)
ν(C–C) 19b	1535 vs	1552 (5)	1552	1548	71.95	0.33	46 (19b)+22 (13)+19 (20b)+10 (18a)
ν(C–F) 2	1486 sh	1487 (6)	1496	1495	14.52	3.96	53 (2)+38 (1)+6 (13)
ν(C–F) 7a	1156 s	1174 (7)	1163	1181	1.62	2.91	53 (7a)+23 (13)+11 (19a)+10 (6b)
ν(C–F) 7b	1138 s	1140 (4)	1141	1135	2.51	0.94	77 (7b)+10 (12)+10 (14)
ν(C–F) 20a	1012 vs	1025 (2)	1013	1018	61.76	0.20	54 (20a)+19 (18a)+16 (8b)+10 (13)
ν(C–F) 20b	984 s	–	979	974	64.01	0.23	60 (20b)+16 (14)+15 (18b))+ 5 [β(OH)]
β(CF) 3	782 s	787 (8)	785	777	2.08	0.10	81 (3)+16 (15)
β(CF) 9a	–	269 (2)	271	271	0.08	0.21	76 (9a)+22 (12)
β(CF) 9b	–	–	283	279	0.45	0.01	82 (9b)+16 (15)
β(CF) 18a	–	–	319	317	0.52	0.02	71 (18a)+21 (19b)
β(CF) 18b	–	295 (2)	315	309	0.54	0.02	57 (18b)+25 (14)+15 (15)
ν(C–C) 1	561 w	562 (100)	563	556	0.25	42.95	63 (1)+32 (3)
β(CCC) 6a	448 w	–	451	442	0.10	7.72	74 (6a)+10 (19b)+8 (9a)+6 (7a)
β(CCC) 6b	448 w	444 (42)	448	438	0.02	7.07	74 (6b)+9 (19a)+8 (7b)+6 (3)
β(CCC) 12	–	601 (10)	600	592	0.17	3.11	62 (12)+26 (7b)+7 (13)
ν(C–O) 13	1310 w, sh	1306 (2)	1319	1312	0.46	0.46	51 (20a)+37 (12)+9 (13)
β(CO) 15	–	–	272	266	1.10	0.46	41 (3)+35 (15)+22 (6b)
(b) Out-of plane vibrations(a"-species)							
τ(CCCC) 4	–	655 (2)	665	650	0.01	0.03	48 (17b)+38 (4)+14 (5)
τ(CCCC)16a	607 w	–	634	612	0.00	0.01	53 (16a)+35 (10b)+13 (5)
τ(CCCC)16b	648 vw	–	655	644	0.08	0.01	57 (17a)+42 (16b)
π(CF) 11	–	370 (23)	363	357	0.11	3.39	72 (11)+26 (5)
π(CF) 17a	–	142 (78)	134	134	0.01	0.05	90 (16b)+7 (17a)
π(CF) 17b	–	150 (2)	137	136	0.01	0.05	89 (4)+5 (17b)
π(CF)10a	–	370 (40)	381	377	0.23	3.46	95 (10a)
π(CF) 10b	–	182 (2)	185	184	0.01	0.04	91 (16a)+6 (10b)
π(CO)5	-	216 (2)	212	210	0.22	0.15	84 (11)+14 (5)
(ii) Vibrations of OH moiety							
(a) In-plane vibrations(a′-species)							
ν(OH)	3583 s	3576 (2)	3805	3581	34.57	100	100 [ν(OH)]
β(OH)	1235 vs	1229 (1)	1256	1253	24.57	0.89	78 (14)+12 [β(OH)]
(b) Out-of plane vibrations(a″-species)							
τ(OH)	–	324 (2)	352	324	32.54	1.25	90 [τ(OH)]

a, b, c ν, β, π, τ, vs, s, w, vw, sh, -: As in Table 2.

Experimental IR and Raman frequencies, corresponding unscaled and scaled frequencies, calculated IR and Raman intensities, potential energy distribution (PED) and vibrational assignments of PBP, and PFP are collected in Tables 2 and 3, respectively. Wilson's notation [40] was used to label different modes having their origin in the aromatic nucleus. A visual comparison of experimental and simulated FT-IR and FT-Raman spectra of PBP is made in Figs. 4 and 5, respectively, whereas corresponding comparison for spectra of PFP is available in Figs. 6 and 7.

The rms error between observed and scaled frequencies, for PBP and PFP is 9.7 and 7.0 cm^{-1}, respectively. Experimental IR and Raman fundamentals agree fairly well with their theoretical counterparts, see Table 2, Figs. 4 and 5 for PBP and see Table 3, Figs. 6 and 7 for PFP. Hence, the vibrational assignments can be made, on the basis of these calculations for PBP and PFP.

The PED presented in Tables 2 and 3 is self-explanatory. But a brief explanation may be in order.

4.4.1. C–C stretching vibrations

Modes 8a and 8b are expected in the range 1500–1650 cm^{-1} in PBP and PFP, as in the case of hexa-substituted benzenes. The higher frequency has about 68% C–C stretching character in the two molecules investigated here. It is to be noted that this fundamental mixes with ∠CCC in-plane bending mode 6b in both PBP and PFP. Further, the PED contribution to this mode, from CBr or CF in-plane bending vibration 18b in these molecules is also noteworthy. This mode derives an additional PED contribution from CO in-plane bending vibration 15 and β(OH) in PBP, whereas these are replaced by CO stretching mode 13 in PFP. The lower frequency in the two molecules is a C–C stretching vibration to the extent of 72-65%. It mixes with mode 6b in PBP, whereas it is replaced by mode 6a in PFP. Other modes mixing with this vibration can be seen from Tables 2 and 3. Thus identified the IR absorptions at 1533 and 1514 cm^{-1} in PBP; 1662R[1] and 1619 cm^{-1} in PFP are ascribed to the modes 8a and 8b, respectively. We find that the mode 8a is greater in frequency than vibration 8b in both PBP and PFP.

Vibrations 19a and 19b are expected in the spectral region 1300-1550 cm^{-1} in this set of molecules. The higher frequency exhibits C–C stretching nature to the extent of 55-47%. The remaining PED

[1] R indicates Raman shift.

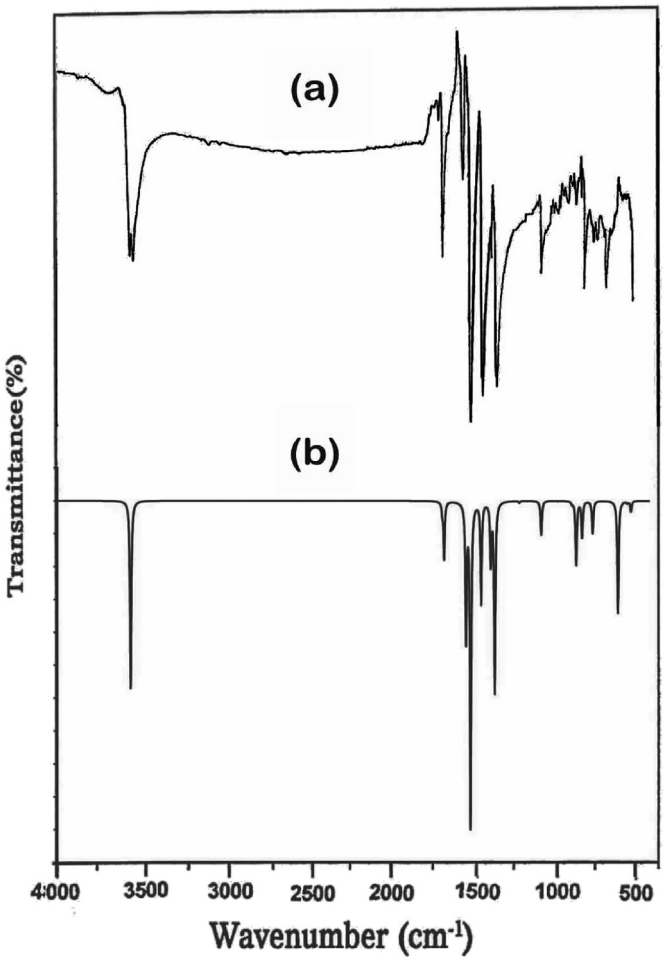

Fig. 4. FT-IR Spectrum of Pentabromophenol (a) Experimental and (b) simulated with DFT/B3LYP/6-311++G (d,p) basis set.

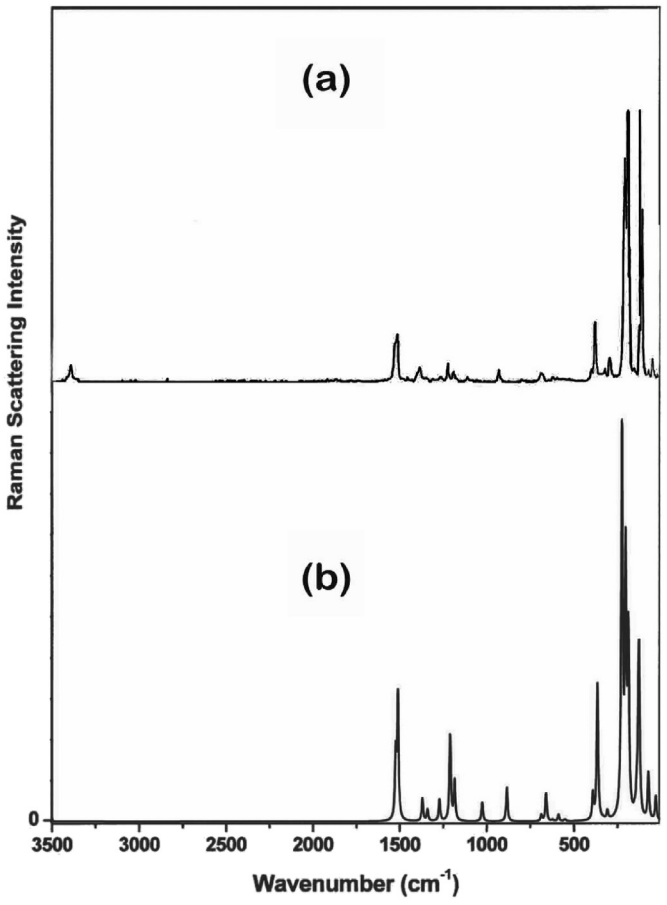

Fig. 5. FT-Raman Spectrum of Pentabromophenol (a) Experimental and (b) simulated with DFT/B3LYP/6-311++G (d,p) basis set.

comes from ν(CO) i.e, mode 13, β(CBr) i.e, vibration 18a, β(OH) and ν(CBr) i.e, fundamental 7b in PBP, whereas the contributing fundamentals, apart from C–C stretching in PFP, are ν(CO) i.e. mode 13, ν(CF) i.e. mode 20b and β(CF) i.e. mode 18a. The lower frequency is a C–C stretching vibration having C–C stretching nature that varies from 53 to 47% in the two molecules. Other modes participating in this vibration can be seen from Tables 2 and 3. Hence, IR bands near 1349 and 1388 cm^{-1} in PBP; 1523 and 1535 cm^{-1} in PFP are ascribed to the modes 19a and 19b, respectively. Thus we can conclude that the frequency of mode 19b is greater in magnitude than the vibration 19a in the two molecules.

Mode 14 in which alternate carbon bonds of the ring, either increase or decrease, appears at 1278 cm^{-1} in PBP, with 73% C–C stretching character. It mixes with β(OH) to the extent of 18%. The IR fundamental around 1356 cm^{-1} in PFP gets 41% PED from mode 14. Hence it is assigned to mode 14 in this molecule. However, it mixes strongly with β(OH) to the extent of 45%.

4.4.2. Ring vibrations

Vibrations 1, 6a, 6b, and 12 are called ring vibrations in benzene and substituted benzenes. These are also known as substituent sensitive modes, as they are sensitive to the nature of substituents on the aromatic nucleus. We have used symmetry coordinates defined in terms of primitive internal coordinates for 6a, 6b, and 12. Hence it is expected that, for a mode say 6a, in the eigen vector matrix the corresponding element should have a large value in comparison with the elements of the other two modes. This is found true, as the corresponding eigenvector elements for the modes 6a, 6b and 12 are 0.745, 0.879 and −0.818, respectively, in PBP. The corresponding elements in PFP are −0.897, −0.919, and −0.944.

Mode 6a is a ∠CCC bending vibration to the extent of 40–74%, where as this quantity ranges from 55 to 74% in mode 6b in PBP and PFP. It is interesting to note that the mode 6a in PBP strongly mixes with CBr stretching vibration 2, whereas such mixing comes from CBr stretching mode 7b, for vibration 6b in this molecule. Thus identified, the Raman shifts at 210 and 222 cm^{-1} are assigned to the modes 6a and 6b in PBP, whereas the IR absorption at 448 cm^{-1}, along with its Raman shift at 444 cm^{-1} is doubly attributed to the vibrations 6a and 6b in PFP.

The main PED contribution to mode 12 comes from the corresponding ∠CCC bending vibration in these molecules. This has considerable mixing from CBr stretching vibration 20a in PBP, while such mixing arises from CF stretching mode 7b in PFP. It is identified near 1000 cm^{-1} in PBP, and at 601 cm^{-1} in PFP.

In mode 1 all the C–C bonds, either increase or decrease in length simultaneously. It is totally symmetric and separated by a large extent from C–H stretching vibrations in benzene. Hence it is a pure C–C stretching vibration in benzene. As these restrictions are removed in the present set of molecules, mode 1 can mix with

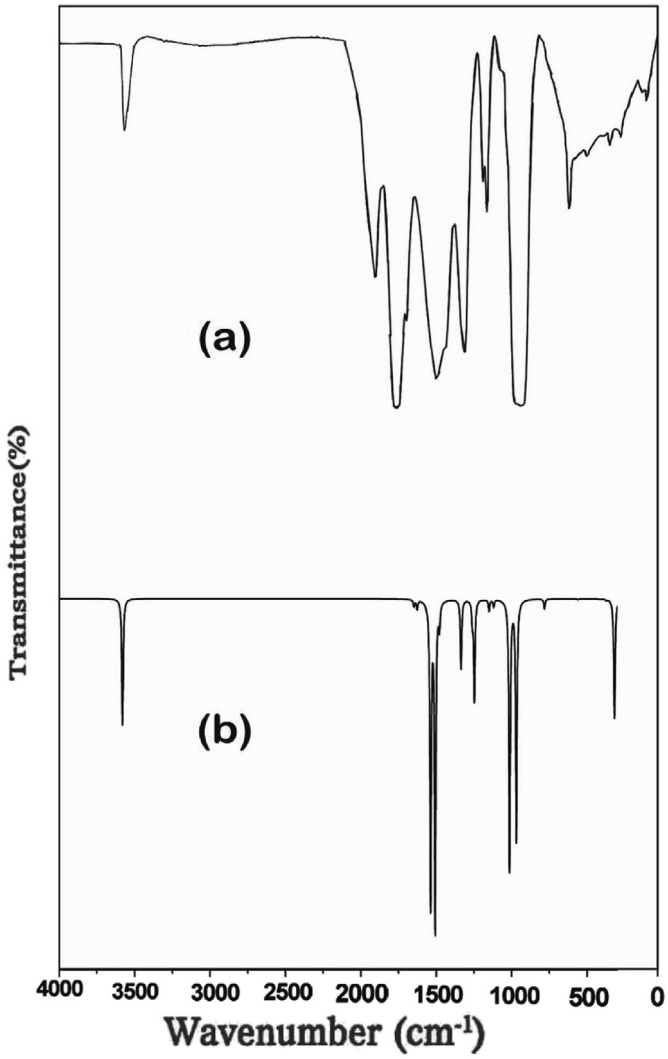

Fig. 6. FT-IR Spectrum of Pentafluorophenol (a) Experimental and (b) simulated with DFT/B3LYP/6-311++G (d,p) basis set.

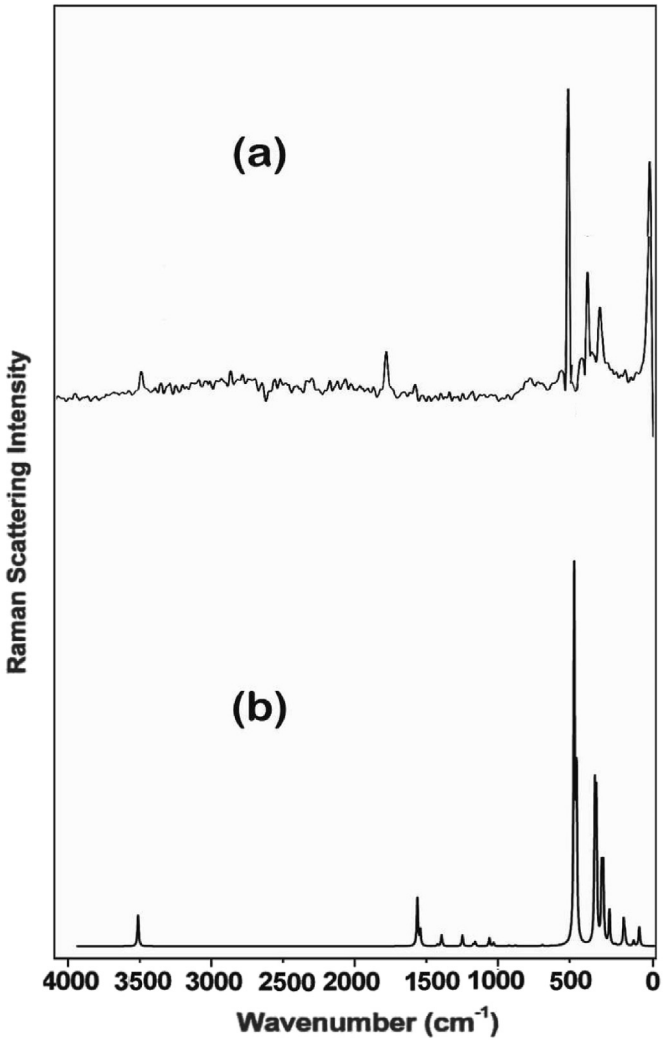

Fig. 7. FT-Raman Spectrum of Pentafluorophenol (a) Experimental and (b) simulated with DFT/B3LYP/6-311++G (d,p) basis set.

several of the bending modes and also with the lower frequencies of the substituent stretching modes. As a result a pure mode cannot be expected corresponding to mode 1 of benzene. The assignment of this fundamental frequency around 1223 and 564 cm^{-1} in PBP and PFP, respectively, is straight forward as it gets 63% of its PED from mode 1 in both the molecules. It mixes with ν(CBr) i.e, mode 2, and β(CF) i.e, mode 3 in PBP and PFP, respectively.

4.4.3. Vibrations associated with C-X bonds (X = Br for PBP and X = F for PFP)

There are 15 vibrations that have their origin in the five bonds of, each of the two molecules, under investigation. These are five C—Br or C—F stretchings, designated 2, 7a, 7b, 20a, and 20b; five C—Br or C—F in-plane bends denoted 3, 9a, 9b, 18a, and 18b; and five C—Br or C—F out-of-plane bends identified 11, 17a, 17b, 10a, and 10b in PBP and PFP. All of them fall below 1000 cm^{-1}. As this is a complicated region of the vibrational spectrum, majority of them cannot be pure. This makes their assignment more difficult. To circumvent this problem and identify each one of them with a specific mode we used the following phase relations among the corresponding elements of eigen vector matrix.

+1	+1	+1	+1	+1	for modes 2, 3 and 11
−1	−1	2	−1	−1	for modes 7a, 9b and 17b
−2	+2	0	−2	+2	for modes 7b, 9a and 17a
+1	−1	−2	−1	+1	for modes 20a, 18b and 10b
−2	−2	0	+2	+2	for modes 20b, 18a and 10a

The +ve and −ve signs indicate increase and decrease, respectively. These statements are approximately true in the case of substituted benzenes under investigation due to lowering of symmetry. However it may still be possible that many of the vibrations may be determined to a large extent by one particular phase relation. In that case it can be correlated with the benzene mode, which is best approximated by that phase relation. Patel at al [37] used this criterion for the assignment of substituent sensitive modes in dihalogenated benzenes. In this way the absorptions near 237R[1],

376 (cal.val)[2], 776, 682, 557, 631, 140R, 140R, 152R, 152R, 152R, 38 (cal.val), 42 (cal.val), 320R, and 347Rcm^{-1}are ascribed to the modes 2,7a, 7b, 20a, 20b, 3, 9a, 9b, 18a, 18b 11, 17a, 17b, 10a, and 10b, respectively in PBP, as ν(CBr) vibrations get 51–72% PED; β(CBr) modes obtain 51–97% PED; and π(CBr) fundamentals draw 74–97% PED, from the corresponding modes. Mixing of all the above 15 vibrations with other fundamentals can be understood from Table 2. It is important to note that Faniran [4] attributed the vibrations around 685(ν_{11}), 670(ν_{12}), 634(ν_{14}), 560(ν_{15}), and 370 (ν_{16}) to the five ν(C–Br) modes, whereas those near 246(ν_{19}), 225(ν_{20}), 173(ν_{21}), 156(ν_{22}), and 133 (ν_{23}) to the five β(CBr) vibrations, while the absorptions at 211(ν_{29}), 109(ν_{30}), and 88 (ν_{31}) to the three, π(CBr) fundamentals out of five (note that ν_{32} and ν_{33} modes representing π(CBr) vibrations were not observed by Faniran). It can be seen that, majority of these assignments differ from the present assignments made on the basis of DFT normal coordinate analysis. This underlines the need for a rigorous theoretical analysis of vibrational frequencies for their accurate assignments. Following the same procedure vibrational assignment of corresponding modes in PFP was made. The nature of these vibrations in terms of mixing of PED can be read from Table 3.

4.4.4. Vibrations of COH moiety

There are six vibrations associated with COH moiety. These are: ν(CO), β(CO), π(CO), ν(OH), β(OH), and τ(OH). The bands at 3530, and 3583 cm^{-1} are due to ν(OH), in PBP, and PFP, respectively. They are pure as each one of them gets 100% PED from the corresponding vibration. The band at 1192 cm^{-1} attributable to β(OH) in PBP appears near 1235 cm^{-1} in PFP. However, it is dominated by PED from CC stretching mode 14 in both the molecules. The vibration τ (OH), in PBP and PFP is located at 401R and 324R cm^{-1}, respectively. As seen from Tables 2 and 3, mixing of this vibration with other modes is negligibly small in these molecules. The assignment of C–O stretching vibration in PBP deserves special mention as it does not align with expectations. In alcohols it should appear in the range 1020–1050 cm^{-1} according to Varsanyi [41], whereas Faniran [4] expects it around 1280 cm^{-1} (ν_7) in agreement with its assignment in phenol and its pentahalo derivatives. DFT calculations presented here negate both these expectations and predict it at 925 cm^{-1}. This low value of its frequency can be traced to its mixing with lower frequencies ν (CBr) 20a to the extent of 38% and β (∠CCC) 6b to the extent of 42%. It is to be noted that the band at 1280 cm^{-1} (our value is 1278 cm^{-1}) has been assigned to mode 14 in section 4.4.1. This assignment of ν(CO)13 is similar to that of corresponding fundamental in Pentachlorophenol [7].

Assignment of ring torsions in 4, 16a, 16b, PBP and PFP can be understood by referring to the PED Tables 2 and 3.

5. Conclusions

From the above investigations the following conclusions are arrived at.

(i) Both PBP and PFP posses a two-fold potential barrier that hinders internal rotation around the C–O bond. Both the molecules are planar with C_S point group symmetry, attaining lowest energy at 0° rotational angle around C–O bond.
(ii) Theoretically determined structure parameters agree very well with their experimental counterparts for PBP and with related molecules for PFP.
(iii) Unambiguous vibrational assignments are made for PBP, and PFP, using PED, and eigenvectors, for the first time. Symmetry-forbidden mixing of PED is not observed in the two molecules investigated.
(iv) There is a good agreement between the experimental and calculated frequencies for the two molecules. Experimental IR and Raman spectra agree fairly well with their computed spectra for PBP, and PFP.
(v) DFT calculations made for dimers of PBP and PFP substantiate the existence of inter-molecular hydrogen bond in both the dimers. Further, both the dimers have C_1 symmetry.

[2] cal.val. indicates calculated value.

Acknowledgements

The authors sincerely acknowledge the University Grants Commission, New Delhi, India (No. F.530/24/DRS-II/2015 (SAP)) for having granted financial support under SAP-DRS-II. The authors are also thankful to Sophisticated Analytical Instrumentation Facility (SAIF), IIT Madras, Chennai, India, for spectral measurements. First two authors (PVR and KSS) are grateful to the management of S R Engineering College (Autonomous), Warangal, India, for permitting them to undertake this research work.

References

[1] C.J. Weinman, G.C. Decker, J.H. Bigger, Insecticidal sprays and dusts for control of Grasshoppers, J. Econ. Entomol. 40 (1947) 91–97.
[2] C.N. Smith, D. Burnett, Effectiveness of repellents applied to clothing for protection against salt-marsh mosquitoes, J. Econ. Entomol. 42 (1949) 439–444.
[3] J. Ham, H. Lee, Fu-Ming Tao, Molecular structures and properties of the complete series of bromophenols: density functional theory calculations, J. Phys. Chem. 109 (2005) 5186–5192.
[4] J.A. Faniran, Vibrational spectra and torsional barriers of pentachloro and pentabromophenols, Spectrochim. Acta, Part A 35 (1979) 1257–1264.
[5] J.A. Faniran, Vibrational spectra and torsional barrier of pentafluorophenol, J. Fluorine Chem. 12 (1978) 345–357.
[6] R. Betz, P. kleifers, P. Mayer, 2, 3, 4, 5, 6-pentabromophenol, Acta Crystallogr. 64 (sup1 to sup5) (2008) 01921.
[7] K. Srishailam, P. Venkata Ramana Rao, L. Ravindranath, B. Venkatram Reddy, G. Ramana R Rao, Experimental and theoretical determination of structural and vibrational properties of Pentachlorophenol and pentachlorothiophenol, J. Mol. Struct. 1178 (2019) 142–154.
[8] M.J. Frisch, G.W. Trucks, et al., Gaussian 09, Revision B.01, Gaussian, Inc., Wallingford CT, 2010.
[9] A.D. Becke, Density-functional thermochemistry. III. the role of exact exchange, J. Chern. Phys. 98 (1993) 5648–5652.
[10] C. Lee, W.T. Yang, R.G. Parr, Development of the colle-salvetti correlation-energy formula into a functional of the electron density, Phys. Rev. B 37 (1988) 785–790.
[11] G. Rauhut, P. Pulay, Transferable scaling factors for density functional derived vibrational force fields, J. Phys. Chem. 99 (1995) 3093–3100.
[12] J. Prashanth, B. Venkatram Reddy, G. Ramana Rao, Investigation of torsional potentials, molecular structure, vibrational properties, molecular characteristics and NBO analysis of some bipyridines using experimental and theoretical tools, J. Mol. Struct. 1117 (2016) 79–104.
[13] M. Karabacak, E. Kose, M. Kurt, FT-Ramana, FT-IR spectra and DFT calculations on monomeric and dimeric structures of 5-fluoro and 5-chloro-salicylic acid, J. Raman Spectrosc. 41 (2010) 1085–1097.
[14] G. Gadaninc, 2,3,4,5,6 –pentafluoroaniline, Acta.Crystallogr. 63 (2007) 2954.
[15] T. Gramstand, S. Hubye, K. Maartmann-Moe, Crystal structure of the hydrogen-bonded complex between pentafluorophenol and trlphenylphosphine oxide, Acta. Chem. Stand. B 40 (1986) 26–30.
[16] T. Sundius, MOLVIB - a flexible program for force field calculations, J. Mol. Struct. 218 (1990) 321–326.
[17] T. Sundius, Scaling of ab initio force fields by MOLVIB, Vib. Spectrosc. 29 (2002) 89–95.
[18] G. Fogarasi, X. Zhou, P.W. Taylor, P. Pulay, The calculation of ab initio molecular geometries: efficient optimization by natural internal coordinates and empirical correction by offset forces, J. Am. Chem. Soc. 114 (1992) 8191–8201.
[19] P. pulay, G. Fogarasi, G. Pongor, J.E. Boggs, A. Vargha, Combination of theoretical *ab initio* and experimental information to obtain reliable harmonic force constants. Scaled quantum mechanical (SQM) force fields for glyoxal, acrolein, butadiene, formaldehyde, and ethylene, J. Am. Soc. 105 (1983) 7037–7047.
[20] J.F. Arenas, I. Lopez Tocon, J.C. Otero, J.I. Macros, Vibrational spectra of methyl pyridines, J. Mol. Struct. 476 (1999) 139–150.
[21] Z. Latajka, W.B. Person, K. Morokuma, An ab initio calculation of the infrared spectrum and tautomerism of guanine, J. Mol. Struct. 135 (1986) 253–266.
[22] G. Kereztury, S. Holly, G. Besenyel, J. Varga, A. Wang, J.R. Durig, Vibrational

spectra of monothiocarbamates-II. IR and Raman spectra, vibrational assignment, conformational analysis and ab initio calculations of S-methyl-N,N-dimethylthiocarbamate, Spectrochim. Acta, Part A 49 (1993) 2007–2026.
[23] G. Kereztury, J.M. Chalmers, in: P.R. Griffith (Ed.), Raman Spectroscopy : Theory in Hand Book of Vibrational Spectroscopy vol. 1, John Wiley & Sons, New York, 2002, pp. 71–87.
[24] Y. Umar, J. Tijani, Density Functional Theory study of the rotational barriers conformational preference, and vibrational spectra of 2-formylfuran and 3-formylfuran, J. Struct. Chem. 56 (2015) 1305–1312.
[25] B.J. Lynch, D.G. Truhlar, How well can hybrid Density Functional Methods predict transition state geometries and barrier heights? J. Phys. Chem. 105 (2001) 2936–2941.
[26] G.E. Campagnaro, J.L. Wood, The vibrational spectra and origin of torsional barriers in some aromatic systems, J. Mol. Struct. 6 (1970) 117–132.
[27] F.R. Jensen, C.H. Bushweller, Separation of conformers. II. Axial and equatorial I isomers of chlorocyclohexane and trideuteriomethoxycyclohexane, J. Am. Chem. Soc. 91 (1969) 3223–3225.
[28] B. Liu, A.D. McLean, Accurate calculation of the attractive interaction of two ground state helium atoms, J. Chem. Phys. 59 (1973) 4557–4558.
[29] S.F. Boys, F. Bernardi, Calculation of small molecular interactions by differences of separate total energies – some procedures with reduced errors, Mol. Phys. 19 (1970) 553.
[30] S. Simon, M. Duran, J.J. Dannenberg, How does basis set superposition error change the potential surfaces for hydrogen bonded dimers? J. Chem. Phys. 105 (1996) 11024–11031.
[31] J.B. Foresman, A. Frisch, Exploring Chemistry with Electronic Structure Methods, third ed., Gaussian Inc., Wallingford CT USA, 2015, p. 440.
[32] T. Steiner, C–H···O hydrogen bonding in crystals, Crystallogr. Rev. 9 (2003) 177–228.
[33] T. Steiner, G.R. Desiraju, Distinction between the weak hydrogen bond and the vander W Waals interaction, Chem. Commun. (1998) 891–892.
[34] G.R. Desiraju, C–H…O and other weak hydrogen bonds.From crystal engineering to v virtual screening, Chem. Commun. (2005) 2995–3001.
[35] F. Biegler-kö nig, Jens schö nbohm , update of the AIM2000-program for atoms in M molecules, J. Comput. Chem. 23 (2002) 1489–1494.
[36] A. Kuwae, K. Machida, Vibrational spectra of nitrobenzene-d_0, p-d and $-d_5$ and normal vibrations of nitrobenzene, Spectrochim. Acta, PartA 35 (1979) 27–33.
[37] N.D. Patel, V.B. Kartha, N.A. Narasimham, Vibrational spectra of dihalogenated benzenes. I. in-plane vibrations, J. Mol. Spectrosc. 48 (1973) 185–201.
[38] D. Vijaya Kumar, V. Ashok Babu, G. Ramana Rao, G.C. Pandey, Vibrational analysis of substituted anilines, anisoles and anisidines, part I. Vibrational spectra and normal coordinate analysis some nitro compounds, Vib. Spectrosc. 4 (1992) 39–57.
[39] E.B. Wilson Jr., A method of obtaining the expanded secular equation for the vibration frequencies of a molecule, J. Chem. Phys. 7 (1939) 1047–1052, 9 (1941) 76-84.
[40] E.B. Wilson Jr., The normal modes and frequencies of vibration of the regular plane hexagon model of the benzene molecule, Phys. Rev. 45 (1934) 706–714.
[41] G. Varsanyi, Assignments for Vibrational Spectra of Seven Hundred Benzene Derivatives, vol. 1, Adam Hilger London, 1974, pp. 27–29, table 2.